

Novel Tube-like $Y_2Sn_2O_7:Tb^{3+}$ Crystals: Hydrothermal Synthesis and Photoluminescence Properties

Jinyu Yang,¹ Yuchang Su,^{*1} and Lijian Li^{1,2}

¹School of Materials Science and Engineering, Central South University, Changsha 410083, P. R. China

²College of Mechanical Engineering, Hunan University of Technology, Zhuzhou 412008, P. R. China

(Received November 12, 2009; CL-090998; E-mail: ychs@mail.csu.edu.cn)

Novel tube-like $Y_2Sn_2O_7:Tb^{3+}$ crystals with pyrochlore structure have been successfully synthesized via a hydrothermal route. The experimental results show that ammonia plays a key role in the fabrication of $Y_2Sn_2O_7:Tb^{3+}$ with tube-like morphology. The photoluminescence spectra indicate that the tube-like $Y_2Sn_2O_7:Tb^{3+}$ crystals emit strong green light at 543 nm under UV excitation. The growth mechanism of tube-like $Y_2Sn_2O_7:Tb^{3+}$ crystals is proposed.

Lanthanide stannates ($Ln_2Sn_2O_7$, $Ln = Y$ and $La-Lu$) with pyrochlore structure have attracted much interest in recent years for a wide variety of properties and applications.¹⁻⁶ As is known, the crystallite size and morphology can influence the properties of materials.⁷ To date, many efforts have been devoted to the controlled synthesis of $Ln_2Sn_2O_7$ with various morphologies and sizes. Lu et al. have prepared a series of $Ln_2Sn_2O_7$ nanocrystals, which display irregular shapes and agglomerates.² Irregular morphology is the common character of solution-synthesized $Ln_2Sn_2O_7$ nanocrystals.^{3,8} Moon et al.⁹ and Fu et al.⁴ have reported a hydrothermal approach for the synthesis of $La_2Sn_2O_7:Eu^{3+}$ micrometer-sized spheres assembled with nanocrystals, which emitted strong orange-red light under UV excitation. Similar $Y_2Sn_2O_7$ crystals with sphere morphology have been produced.¹⁰ $La_2Sn_2O_7$ nanorods have been fabricated in ethanol solvent, and the emission intensity of the nanorods was stronger than that of the phosphor with other morphologies.¹¹ Zhu et al.¹² have synthesized flower-like $La_2Sn_2O_7$ nanostructures assembled with nanorods. Zeng et al.⁵ have successfully synthesized $La_2Sn_2O_7$ nanocubes with good photocatalytic activities through hydrothermal route. 3D octahedral $La_2Sn_2O_7:Eu^{3+}$ crystals with high luminescent intensity have been fabricated.¹³ However, to our knowledge, no reports have been published on the synthesis of tube-like $Ln_2Sn_2O_7$. Herein, the fabrication of $Y_2Sn_2O_7:Tb^{3+}$ crystals with tube-like morphology via hydrothermal process was presented. A possible growth mechanism and photoluminescence of the tube-like crystals were also investigated.

$Y_2Sn_2O_7:Tb^{3+}$ was synthesized via a hydrothermal route using $Y(NO_3)_3 \cdot 6H_2O$, $Tb(NO_3)_3 \cdot 6H_2O$, and $SnCl_4 \cdot 5H_2O$ as starting reagents, and the atomic ratio of $Tb^{3+}:Y^{3+}$ was fixed at 5:95. The pH of the solution was adjusted to 12.5 by using strong aqueous ammonia or 4 mol L^{-1} NaOH solution. The synthesis procedure was similar to that described in a previous paper¹³ except that the starting reagents and mineralizers were different. The as-synthesized $Y_2Sn_2O_7:Tb^{3+}$ sample obtained in aqueous ammonia is denoted as S1, and the sample prepared in NaOH solution is denoted as S2.

Figure 1a shows the XRD patterns of samples obtained using different mineralizers. All the diffraction peaks in the XRD patterns can be indexed as the pyrochlore structure of

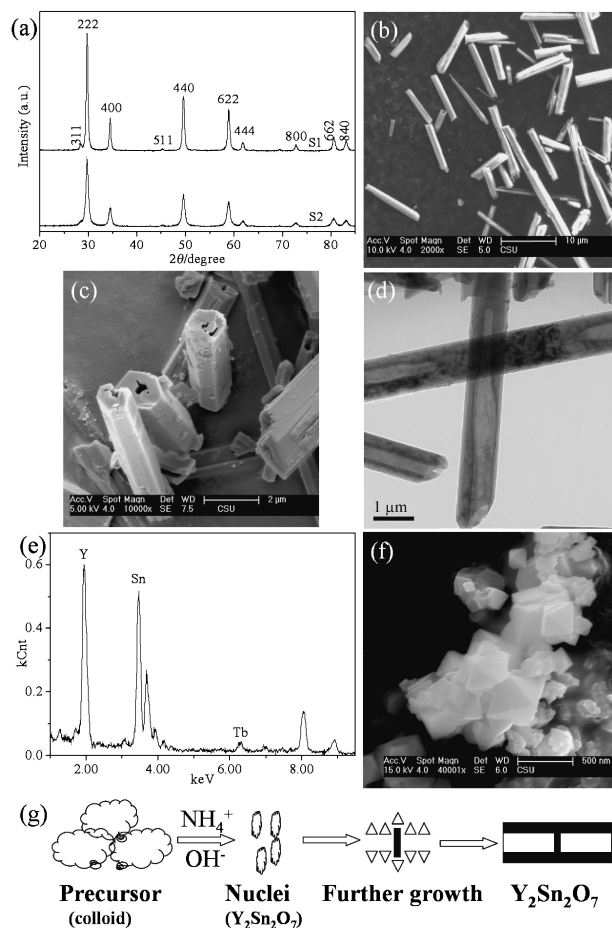


Figure 1. (a) XRD patterns of the as-prepared $Y_2Sn_2O_7:Tb^{3+}$ samples, (b–c) SEM images of S1, (d) TEM image of S1, (e) EDS spectrum of S1, (f) SEM image of S2, and (g) schematic illustration of the formation mechanism of tube-like $Y_2Sn_2O_7:Tb^{3+}$ crystals.

$Y_2Sn_2O_7$ (JCPDS 82-0662) with space group of $Fd\bar{3}m$ (No. 227). No peaks of impurities can be detected. The lattice parameters were calculated as 10.3963, and 10.3975 Å for S1 and S2, respectively. They are slightly larger than that of the JCPDS reference data, indicating that Tb^{3+} ions were introduced into the $Y_2Sn_2O_7$ lattice. It can be seen from Figure 1a that the intensity of the diffraction peaks of S1 is stronger than that of S2, revealing a high crystallinity and grain size of S1.

Figures 1b–1d show SEM and TEM images of S1. The images in Figures 1b–1d clearly reveal that S1 exhibits hexagonal tubular structure with high yield (Figure 1c). Furthermore, the block region at the center of tubular structures can be observed (Figure 1d). However, when the sample was

synthesized in NaOH solution, the morphology of products dramatically changes to irregular 3D octahedron, as shown in Figure 1f. Besides, Figure 1e shows the EDS spectrum of S1, revealing that the Tb^{3+} ions have entered into $\text{Y}_2\text{Sn}_2\text{O}_7$ crystals. This is in agreement with the result of the lattice constants measurements. Therefore, it can be inferred that ammonia plays an important role in the fabrication of $\text{Y}_2\text{Sn}_2\text{O}_7:\text{Tb}^{3+}$ with tube-like morphology.

Base on the above results, a formation mechanism of the tube-like crystals is proposed, as shown in Figure 1g. When $\text{Y}(\text{NO}_3)_3$ and SnCl_4 were mixed with aqueous ammonia in the initial stage, they reacted with OH^- groups to form $\text{Y}(\text{OH})_3$ and amorphous $\text{Sn}(\text{OH})_4$ precipitations respectively, forming highly disordered colloidal precursor. Meanwhile, $\text{NH}_4\text{NO}_3/\text{NH}_4\text{Cl}$ would also occur in solution. As seeds, $\text{Y}(\text{OH})_3$ clusters with hexagonal structure were first obtained while in a hydrothermal process with temperature elevated. In our case, the amorphous $\text{Y}(\text{OH})_3$ precipitations could dissolve in boiling $\text{NH}_4\text{Cl}/\text{NH}_4\text{NO}_3$ solutions.¹⁴ Due to the high pH, some of the Y^{3+} ions were precipitated as $\text{Y}(\text{OH})_3$ again. Such dissolution and precipitation would allow a dynamic equilibrium to be established. Similarly, under strong alkaline (pH 12.5) and high temperature conditions, parts of amorphous $\text{Sn}(\text{OH})_4$ precipitations could dissolve gently to form soluble $\text{Sn}(\text{OH})_6^{2-}$ species. Subsequently, the Y^{3+} ions in solution would react with $\text{Sn}(\text{OH})_6^{2-}$ species and further form the growth units of $\text{Y}_2\text{Sn}_2\text{O}_7$. These growth unit clusters with critical sizes used as $\text{Y}_2\text{Sn}_2\text{O}_7$ nucleus located preferentially at the circumferential edges of each regular shape seed due to the high density of nucleation sites on it. The sufficient Y^{3+} and $\text{Sn}(\text{OH})_6^{2-}$ in bulk solution were favorable for the nucleation and retained the hexagonal shape of seed. Subsequently, the growth units of $\text{Y}_2\text{Sn}_2\text{O}_7$ could quickly aggregate at the circumferential edges of seeds, and then further grew into crystallites¹⁵ along the (111) orientation.¹⁶ The continuous feeding of growth units on the edges of the crystallite could diffuse and grow into two directions: inner diffusion and diffusion parallel to the (111) orientation. A high concentration of growth units on the diffusion layer will facilitate a rapid diffusion and growth at the two ends rather than at inner. Therefore, the tubular structures could be easily formed. In the present case, ammonia plays the predominant role in the formation of $\text{Y}_2\text{Sn}_2\text{O}_7:\text{Tb}^{3+}$ tubes. The formation mechanism is similar to others reports.^{17,18}

The photoluminescence spectra of the samples are illustrated in Figure 2. The excitation spectra reveal a group of excitation bands in the wavelength region from 300 to 420 nm, which correspond to the f-f transitions of the 4f electronic shell of Tb^{3+} , as shown in Figure 2a. And a weak peak was also observed at 284 nm, ascribed to the $4f^8-4f^75d^1$ absorption band of Tb^{3+} . The prominent peak was centered at 379 nm, which is in agreement with a previous report.¹⁹ The emission spectra of Tb-activated phosphors are shown in Figure 2b. It is noted that the peak at 543 nm originating from $^5\text{D}_4-^7\text{F}_5$ transition has the strongest intensity. Meanwhile, the weak bands at 451 and 469 nm were observed which are attributed to surface oxygen vacancies and defects of the $\text{Y}_2\text{Sn}_2\text{O}_7:\text{Tb}^{3+}$ crystals.²⁰ From Figure 2, it can be seen that the photoluminescence intensity of S1 is somewhat stronger compared with that of S2, which may be attributed to the regular tube-like shape and larger size of $\text{Y}_2\text{Sn}_2\text{O}_7:\text{Tb}^{3+}$.

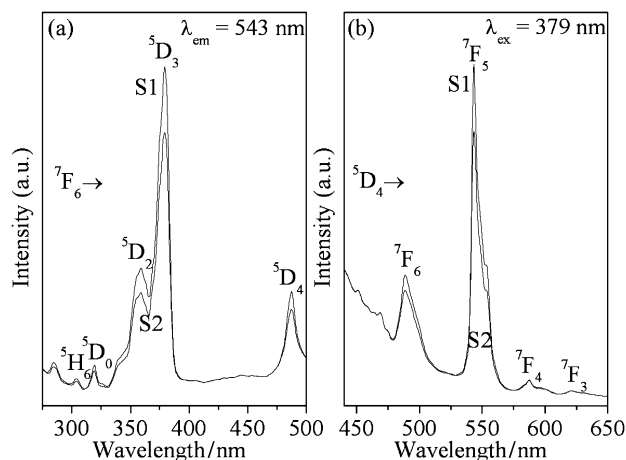


Figure 2. The excitation (a) and emission (b) spectra of the synthesized $\text{Y}_2\text{Sn}_2\text{O}_7:\text{Tb}^{3+}$ samples.

In summary, novel tube-like $\text{Y}_2\text{Sn}_2\text{O}_7:\text{Tb}^{3+}$ crystals have been successfully synthesized via a hydrothermal route. It was found that ammonia played a crucial role in the fabrication of $\text{Y}_2\text{Sn}_2\text{O}_7:\text{Tb}^{3+}$ with tube-like morphology. The possible formation mechanism of tube-like $\text{Y}_2\text{Sn}_2\text{O}_7:\text{Tb}^{3+}$ was discussed. The novel tube-like $\text{Y}_2\text{Sn}_2\text{O}_7:\text{Tb}^{3+}$ displays characteristic typical green emission, which would be a promising green phosphor for applications in lamps and displays.

The authors acknowledge the financial support from Innovation Foundation of China's Ministry of Science and Technology (No. 07C26214301746), and the Graduate degree thesis Innovation Foundation of Central South University (No. 2009bsxt001).

References

- M. A. Subramanian, G. Aravamudan, G. V. Subba Rao, *Prog. Solid State Chem.* **1983**, *15*, 55.
- H. Cheng, L. P. Wang, Z. G. Lu, *Nanotechnology* **2008**, *19*, 025706.
- S. Fujihara, K. Tokumo, *Chem. Mater.* **2005**, *17*, 5587.
- Z. L. Fu, H. K. Yang, B. K. Moon, B. C. Choi, J. H. Jeong, *Cryst. Growth Des.* **2009**, *9*, 616.
- J. Zeng, H. Wang, Y. C. Zhang, M. K. Zhu, H. Yan, *J. Phys. Chem. C* **2007**, *111*, 11879.
- F. Matteucci, G. Cruciani, M. Dondi, G. Baldi, A. Barzanti, *Acta Mater.* **2007**, *55*, 2229.
- J. B. Jackson, N. J. Halas, *J. Phys. Chem. B* **2001**, *105*, 2743.
- S. Nigam, V. Sudarsan, R. Vatsa, J. Ghatak, P. V. Satyam, *J. Phys. Chem. C* **2009**, *113*, 8750.
- J. Moon, M. Awano, K. Maeda, *J. Am. Ceram. Soc.* **2001**, *84*, 2531.
- K. W. Li, H. L. Li, H. M. Zhang, R. Yu, H. Wang, H. Yan, *Mater. Res. Bull.* **2006**, *41*, 191.
- S. M. Wang, G. J. Zhou, M. K. Lu, Y. Y. Zhou, Z. S. Yang, *J. Alloys Compd.* **2006**, *424*, L3.
- H. L. Zhu, D. R. Yang, L. M. Zhu, D. Li, P. Chen, G. Yu, *J. Am. Ceram. Soc.* **2007**, *90*, 3095.
- J. Y. Yang, Y. C. Su, *Mater. Lett.* **2010**, *64*, 313.
- T. Moeller, H. E. Kremers, *Chem. Rev.* **1945**, *37*, 97.
- G. Krueger, C. Miller, *J. Chem. Phys.* **1953**, *21*, 2018.
- S. Murugesan, V. Subramanian, *Chem. Commun.* **2009**, 5109.
- Y. Xia, P. Yang, Y. Sun, Y. Liu, B. Mayers, B. Gates, Y. Yin, F. Kim, H. Yan, *Adv. Mater.* **2003**, *15*, 353.
- L. F. Liang, H. F. Xu, Q. Su, H. Konishi, Y. Jiang, M. Wu, Y. Wang, D. Xia, *Inorg. Chem.* **2004**, *43*, 1594.
- J. S. Liao, B. Qiu, H. S. Lai, *J. Lumin.* **2009**, *129*, 668.
- M. Zhou, J. Yu, S. Liu, P. Zhai, L. Jiang, *J. Hazard. Mater.* **2008**, *154*, 1141.